Dynamics of cortical and corticomuscular connectivity during planning and execution of visually guided steps in humans

Meaghan Elizabeth Spedden[a], Mikkel Malling Beck[a], Timothy O. West[b,c], Simon F. Farmer[d,e], Jens Bo Nielsen[f,g], Jesper Lundbye-Jensen[a]

[a]Department of Nutrition, Exercise and Sports, University of Copenhagen, Copenhagen, Denmark

[b]Wellcome Centre for Human Neuroimaging, UCL Institute of Neurology, London WC1N 3AR, UK

[c]Medical Research Council Brain Network Dynamics Unit, Nuffield Department of Clinical Neurosciences, University of Oxford, Mansfield Road, Oxford OX1 3TH, UK.

[d]Department of Clinical Neurology, The National Hospital for Neurology and Neurosurgery, Queen Square London WC1N 3BG, UK

[e]Department of Clinical and Movement Neurosciences, Institute of Neurology, Queen Square, London WC1N 3BG, UK

[f]Department of Neuroscience, University of Copenhagen, Copenhagen, Denmark

[g]Elsass Foundation, Charlottenlund, Denmark

Running title: Coherence during stepping

Keywords: coherence, EEG, EMG, stepping, walking

Proof and correspondence to:

Meaghan Elizabeth Spedden

Department of Nutrition, Exercise and Sports

University of Copenhagen

Nørre Allé 51, 2200 Copenhagen N, Denmark.

Phone: +45 25 63 94 83, e-mail: msp@nexs.ku.dk

Abstract

The cortical mechanisms underlying the act of taking a step - including planning, execution, and modification - are not well understood. We hypothesized that oscillatory communication in a parieto-frontal and corticomuscular network is involved in the neural control of visually guided steps. We addressed this hypothesis using source reconstruction and lagged coherence analysis of electroencephalographic (EEG) and electromyographic (EMG) recordings during visually guided stepping and two control tasks that aimed to investigate processes involved in (1) preparing and taking a step; and (2) adjusting a step based on visual information. Steps were divided into planning, initiation, and execution phases. Taking a step was characterized by an up-regulation of beta/gamma coherence within the parieto-frontal network during planning followed by a down-regulation of alpha and beta/gamma coherence during initiation and execution. Step modification was characterized by bi-directional modulations of alpha and beta/gamma coherence in the parieto-frontal network during the phases leading up to step execution. Corticomuscular coherence did not exhibit task-related effects. We suggest that these task-related modulations indicate that the brain makes use of communication through coherence in the context of large scale, whole body movements, reflecting a process of flexibly fine-tuning inter-regional communication to achieve precision control during human stepping.

1. Introduction

The ease with which we as adult human beings adjust our steps to avoid an obstacle in our path or step up on a curb obscures the considerable computational complexity underlying these movements. The position of the obstacle or target relative to the body has to be identified, appropriate adjustments to the leg movements have to be selected and planned according to target properties, and then implemented as a complex series of timings and degrees of activation in the many muscles involved (Patla 1997).

These adjustments occur frequently during walking behavior. Walking in a natural environment rarely consists of continuous, steady-state locomotion, but is more often interspersed with goal-directed steps aiming to precisely place the foot on a foothold. Traditionally, walking studies have focused on understanding the steady-state component, while the critical component of taking goal-directed steps and making step adjustments based on visual information about the environment has been overlooked.

Importantly, the neural structures and mechanisms underlying the planning, execution and visually guided modification of goal-directed steps in humans are not well understood. A cortical involvement in goal-directed stepping is supported by a number of studies using single-cell recordings in cats that have identified a network of cortical structures involved in the planning and execution of visually guided modifications to walking comprising the posterior parietal cortex (PPC), premotor cortex (PMC), and primary motor cortex (M1) (Drew and Marigold 2015; Marigold and Drew 2017; Nakajima et al. 2019). The activity modulation patterns observed in these structures during visually guided adjustments to the walking pattern suggest that they are involved in different components of the planning and execution processes.

The PPC may contribute to planning through estimation of target position relative to body position during walking (Andujar et al. 2010; Drew and Marigold 2015; Marigold and Drew 2017). The PMC has been suggested to be involved in the temporal transformation of information about target and body position to motor activity (Nakajima et al. 2019). In primates, the dorsal PMC in particular is of interest based on its role in processing of visual information for movement planning (Hoshi and Tanji 2006, 2007). Evidence

from cats also indicates that the M1 and corticospinal pathway play a central role in the execution of motor activity leading to the appropriate step modification (Beloozerova and Sirota 1993; Drew and Marigold 2015).

Available evidence from human studies, although limited, appears to corroborate the more extensive work in animals. Studies using functional imaging of imagined walking (Hamacher et al. 2015) and recordings of electroencephalographic activity (EEG) during real walking movements (Wagner et al. 2014; Varghese et al. 2016; Nordin et al. 2019) suggest that the PPC and PMC are engaged during stepping requiring visual guidance of foot placement. Moreover, previous work using transcranial magnetic stimulation (TMS), as well as using electroencephalographic (EEG) and electromyographic (EMG) recordings, also suggests that visual guidance of foot placement during walking is accompanied by increased involvement of M1 and the corticospinal pathway (Schubert et al. 1999; Jensen et al. 2018; Spedden, Choi, et al. 2019).

Most previous work has focused on the contribution of brain structures in terms of whether activity in any given brain area is modulated by task, while there is a lack of information about how these structures *interact* to form functional networks. This functional integration of information between specialized areas is important as an underlying principle for how the CNS organizes emergent behavior (Friston 1994). An important mechanism for communication in functional networks involves neural oscillations and their synchronization (Lopes da Silva 2013; Fries 2015), which can be quantified through functional connectivity analyses based on the correlational structure between signals.

We aimed to study oscillatory functional connectivity during discrete, visually guided steps within a cortical network comprising PPC, PMC, and M1; and in a corticospinal network between M1 and the spinal motor neurons controlling an ankle muscle important for human gait, *tibialis anterior* (TA). We investigated step planning, initiation, and execution, and compared the visually guided steps to two control tasks: standing quietly and viewing the same visual stimuli, designed to isolate the act of taking a step, and self-guided steps (i.e., no visual information guiding foot placement), designed to isolate the modification of the step based on visual information.

We expected that: (1) The act of taking a step is characterized by modulations of connectivity in the parieto-frontal network throughout the step phases, indicating the involvement of communication within the network in planning and execution processes. We also expected that planning, initiation, and execution phases exhibit distinct connectivity modulations (Drew and Marigold 2015). (2) Step modifications based on visual information are characterized by connectivity modulations in the parieto-frontal network primarily in planning phases, indicating that the major involvement of this network is in the stages leading up to movement initiation. This hypothesis is based on the ballistic model of stepping, which suggests that step trajectory may to a large extent be determined before the foot is lifted (Day and Bancroft 2018). (3) Functional connectivity in a corticomuscular network is greater during visually guided step execution than during the corresponding periods of the control tasks, indicating greater involvement of the corticospinal pathway (Jensen et al. 2018; Spedden, Choi, et al. 2019).

2. Methods

2.1 Participants

Thirty-one healthy adult participants were recruited through social media bulletins and convenience sampling. Data from seven participants was excluded due to either technical problems during recording (n=5) or excessively noisy EEG signals (i.e., with irregular artifacts that were not well isolated by independent components analysis, see below; n=2), resulting in a sample of 24 participants (mean and standard deviation for age: 26 ± 4 years, age range 21-35 years, 9 female).

Seventeen participants were classified as right leg dominant based on self-reporting of the leg with which they preferred to take a step. Experiments were performed in accordance with the Declaration of Helsinki and the study was approved by ethics committee for the Capital Region of Denmark (H-17019671). All participants provided written, informed consent before participating in experiments.

2.2 Tasks

Participants performed four blocks of measurements each containing the task of interest and two control tasks, presented in a pseudo-randomized order. Each task was repeated consecutively for 45 trials in each block, resulting in a total of 180 trials per task (i.e., 4 blocks containing 45 trials of each of the three tasks). The three tasks were: (1) visually guided steps, (2) self-guided steps, and (3) standing and watching visual cues without stepping. Participants were familiarized with the three tasks in a short training block containing 5 trials of each task.

In visually guided stepping, participants took single, goal-directed steps aiming to hit virtual visual targets projected on to the wall in front of them with a cursor tied to their foot position (Figure 1A). For practical reasons related to the setup of the motion capture system, all steps were performed with the right leg. We checked whether task performance was affected by leg dominancy, and the results demonstrated that stepping precision (error) did not differ between right- and left leg dominant participants (see Results).

The screen projected on to the wall in front of the participant displayed stepping targets as red squares (5 x 5 cm), and a blue circular cursor representing the stepping foot position at specific time points. Participants controlled the blue circle with their foot by way of a motion capture system (see section Motion Capture), with target position controlled using a custom-made MATLAB program. The goal of the task was to take a step forward, placing the foot precisely so that the blue circle hit the center of the target. Participants were instructed to take a normal step and only to adjust the length of the step. The required step length was visually represented as the vertical distance between the starting point, marked on the screen with an 'x', and the target center. Note that we projected the target onto the wall instead of the floor with the goal of minimizing neck EMG artifacts in EEG signals that could arise from participants looking down.

At the beginning of each trial, the blue circle and target were presented. After hearing a beep serving as the *go* signal (1 second after target presentation), participants took a single step forward aiming to hit the target. The step ended with the trailing foot placed alongside the stepping foot. Participants were allocated 4 seconds to complete the step and were allowed to initiate the movement at their own pace, so long as it was completed within the time interval.

During the execution of the step, the blue circle was hidden to prevent online adjustments of leg trajectory, i.e., the target, but not the foot, was visible. After the step was completed, the foot endpoint position (blue circle) was displayed, giving participants feedback on endpoint and endpoint error, and a second sound (4 seconds later) indicated that participants were to return to the starting position.

Target distance from starting position was individually calibrated to the preferred step length of each participant, which was measured prior to the start of the recordings as the mean length of three self-guided steps (mean and standard deviation across all participants: 57.04 ± 8.5 cm). To encourage continued use of visual feedback, step length was drawn randomly from three possible lengths: preferred step length and preferred length ± 5 cm in the anterior-posterior direction. Participants were not made aware of the possible target placements and were simply instructed to hit the targets as precisely as possible.

Visually guided stepping was compared with two control conditions: standing and watching, where the participant stood (quiet stance) and viewed the same visual stimuli, and self-guided stepping, where foot placement was not guided by any visual information, i.e., there was no target or augmented feedback on performance (Figure 1C).

In the stand and watch task, participants were presented with the same target and blue circle as in the visually guided stepping task, but did not take steps. Specifically, they viewed a target and blue circle (stepping foot) and heard the go signal; they then stood quietly while watching the blue circle appear around the target as in a visually guided step. The comparison between standing and watching and visually guided stepping was intended to highlight step-related functional connectivity. An alternative design in this context could be to compare quiet standing and stepping, both without visual stimuli; however, we chose to prioritize recording a greater number of trials at the expense of including a fourth condition, a trade-off that was necessary given the long duration of the experiments (3-4 hours).

In the self-guided steps, participants took a single step forward after they heard the *go* sound. All steps were performed with the right leg as for visually guided steps. Participants were instructed to take a normal step forward and were allocated 4 seconds to complete the step. A second sound indicated that they were to return to the starting position as in the visually guided stepping task. No visual information was provided regarding foot placement, thus the comparison between visually guided and self-guided steps should reflect connectivity related to the aspect of visual guidance of the step.

2.3 Motion capture

Motion capture was used to track the 3D position of the stepping foot using retro-reflective markers (12 mm diameter) placed on the right toe (fifth metatarsal head) and heel (calcaneus). Kinematic data was collected at 100 Hz using 8 OptiTrack FLEX infrared cameras and Motive software (7.3.1). Data was streamed to MATLAB, where a custom-made script controlled the stimulus presentation.

2.4 EEG and EMG recordings

EEG was recorded continuously throughout each block using ActiveTwo BioSemi hardware and 64 pin electrodes. Electrodes were arranged in a head cap according to the 10-20 system. EMG was recorded from the right TA (distance between electrodes ~1.5 cm).

EEG and EMG data were sampled at 2048 Hz using ActiView software (version 6.05). This system contains an anti-aliasing filter at the amplifier which is applied at the Nyquist frequency (BioSemi, The Netherlands). The online reference in the BioSemi system is constructed from the Common Mode Sense active electrode and Driven Right Leg passive electrode. Electrode offsets were kept under ~25 mV during recordings. Participants were instructed to relax face and neck muscles as much as possible during the experiments to limit the effects of craniofacial muscle artifacts contaminating EEG signals. We monitored EEG signals online and reminded participants to relax when necessary. To synchronize the electrophysiological and kinematic data, TTL pulses were sent from the MATLAB program controlling stimulus presentation to Motive and ActiView at the beginning and end of each trial.

2.5 Data analysis

2.5.1 Kinematics

Kinematic data from markers on the toe and heel were used to determine the timing of toe-offs and heel strikes, respectively. Toe-off was defined as the time when toe marker velocity in the anterior-posterior direction increased over 10 % of maximum velocity, and heel strike as the time when heel marker velocity fell below 10 % of maximum velocity. Thresholds were defined during piloting by comparing kinematics with events extracted from foot-switches.

Performance on the visually guided stepping task was measured as the mean absolute error in the anterior-posterior direction, i.e., the mean distance between the foot endpoint and center of the target across trials. We removed outlier trials defined as ± 3 standard deviations from the mean for each participant. We also assessed whether visually- and self-guided steps differed in how dynamically the movements were executed

as a potential confounding factor. To do this, we compared mean absolute peak acceleration in the period from toe-off to heel strike in the two stepping conditions.

2.5.2 EEG and EMG pre-processing

Data analysis was performed in MATLAB (R2019a). We used EEGlab (v2019) to pre-process our data. We initially removed EEG channels showing large amplitude deflections and/or consistent EMG activity from face and neck muscles and interpolated them using spherical splines. An average of 5.2 ± 1.6 channels were removed from each block of recordings, typically from around the neck. EEG signals were re-referenced to common average, high pass filtered at 1 Hz with an FIR filter (transition band width 1 Hz, 6761 points), then re-sampled to 512 Hz. Data was epoched from 500 ms prior to stimulus presentation (corresponding to 1500 ms before the *go* signal for self-guided steps) to 4 seconds post stimulus presentation to focus the following analysis on the step forward (and corresponding period for stand and watch).

EMG was pre-processed in a corresponding manner and merged with the EEG data to one data set. EMG channels were re-referenced to a bipolar montage, high-pass filtered at 5 Hz (FIR filter, transition band width 2 Hz, 3381 points) to minimize low-frequency drifts, re-sampled and epoched. EMG signals were rectified to enhance information about the timing of motor unit potentials in the signals (Halliday and Farmer 2010).

Epochs where many EEG channels exhibited large, irregular deflections indicating noise were rejected before running independent components analysis (ICA) on the EEG only using the *runica* algorithm. We adjusted the rank of the data to account for interpolated channels and average referencing. Line noise was reduced using the Cleanline plugin (Mullen 2012) on component time courses. ICA was performed on data from each participant over all conditions. We rejected components from the data if they exhibited spectral, topographical and/or temporal features indicating that they were dominated by artifact from eye blinks/saccades, muscle activity, bad channels (i.e. focal topographies suggesting lack of correlation with

neighbor channels) or rare events. Any components exhibiting high amplitude movement-related deviations (identified by their temporal relation to toe-off and heel-strike) were also removed.

We rejected components based on visual inspection as automated methods are not currently able to accurately isolate artifacts without supervision (Chaumon et al. 2015). A total of 32 ± 7 components were retained from each participant. Finally, we inspected EMG signals and rejected any epochs exhibiting excessive noise, i.e. remaining baseline wandering and/or large deflections, or indications of stepping at inappropriate times. The average number of epochs retained (including all three conditions) was 508 ± 12.5 (94 % of total number of trials).

In a dynamic task like stepping, EEG signals can be affected by movement artifacts. Although there is not yet a consensus on the best way to mitigate these effects, we applied the following strategies during pre-processing: we used an average reference, which should lessen movement artifacts based on the similarity of artifacts across channels (Snyder et al. 2015); we high-pass filtered the data at 1 Hz to remove slow drifts; and we visually inspected epochs and independent components for signs of large movement-related deflections and rejected contaminated data. Also of note, the self-guided stepping task provided a control condition with the same degree of movement as the visually guided stepping task. Finally, we used a source localization technique that we expected to lessen movement artifact effects on the basis that large common artifacts cannot be explained by local brain sources (Litvak et al. 2010) (see following paragraphs).

To verify the quality of our data after pre-processing, we performed time-frequency analysis on the Cz electrode for the two stepping conditions to confirm the presence of event-related desynchronization (ERD) during the step. Time-frequency representations were calculated using FieldTrip scripts included in SPM ('mtmconvol' function; df = 2; 0.5 s time window; steps of 0.25 s). Single time-frequency spectra (not shown) and grand-average (Supplementary Figure 1A) suggested the presence of a robust mu/alpha and beta ERD from the time of the *go* signal and onwards. For comparison, the grand average time-frequency spectrum for the standing and watching condition is also shown (Supplementary Figure 1B).

2.5.3 Analysis periods

We then separated the data into new data sets to analyze the four time periods of interest: early planning, late planning, initiation, and execution for each of the three tasks (Figure 1C). The division of the step into these phases was based on selecting conceivably key time points related to the visual stimulus and movement with the goal of understanding the temporal progression of activity throughout the step. Thus, the definition of the four phases aimed to capture the temporal development as opposed to defining necessarily distinct processes (e.g., processes occurring during early and late planning and/or late planning and initiation may overlap).

Early planning was defined as the period from 100-600 ms after the visual stimulus (target) was presented. Note that for the self-guided stepping task, this corresponded to a period of standing with no visual stimulus. Late planning was defined as the period from 100-600 ms after the go signal (beep) for each of the three tasks.

Initiation and execution were demarcated based on toe-off and heel-strike events, respectively. Initiation was defined as -500 to 0 ms prior to toe-off, corresponding to pre-step postural adjustments (Day and Bancroft 2018). Mean time between the 'go' signal and toe-off was 1.84 ± 0.1 s for self-guided steps and 1.73 ± 0.2 s for visually guided steps. This entails that there were ~1.2 seconds from the start of late planning to the start of initiation. The relatively long reaction time likely reflects that we encouraged participants to take their time to initiate a step forward within the allocated four seconds. This was done to encourage as natural a movement pattern as possible.

Execution was defined from -500 to 0 ms prior to heel-strike, corresponding to the swing phase. We defined the execution phase prior to heel strike rather than after toe-off to ensure that we did not include artifacts due to the heel strike impact in the signals.

This duration was chosen based on inspection of individual swing phase durations suggesting that most were ~500 ms. For the standing and watching task, we used the mean times for toe-off and heel-strike during visually guided steps to select periods of standing for comparison with stepping.

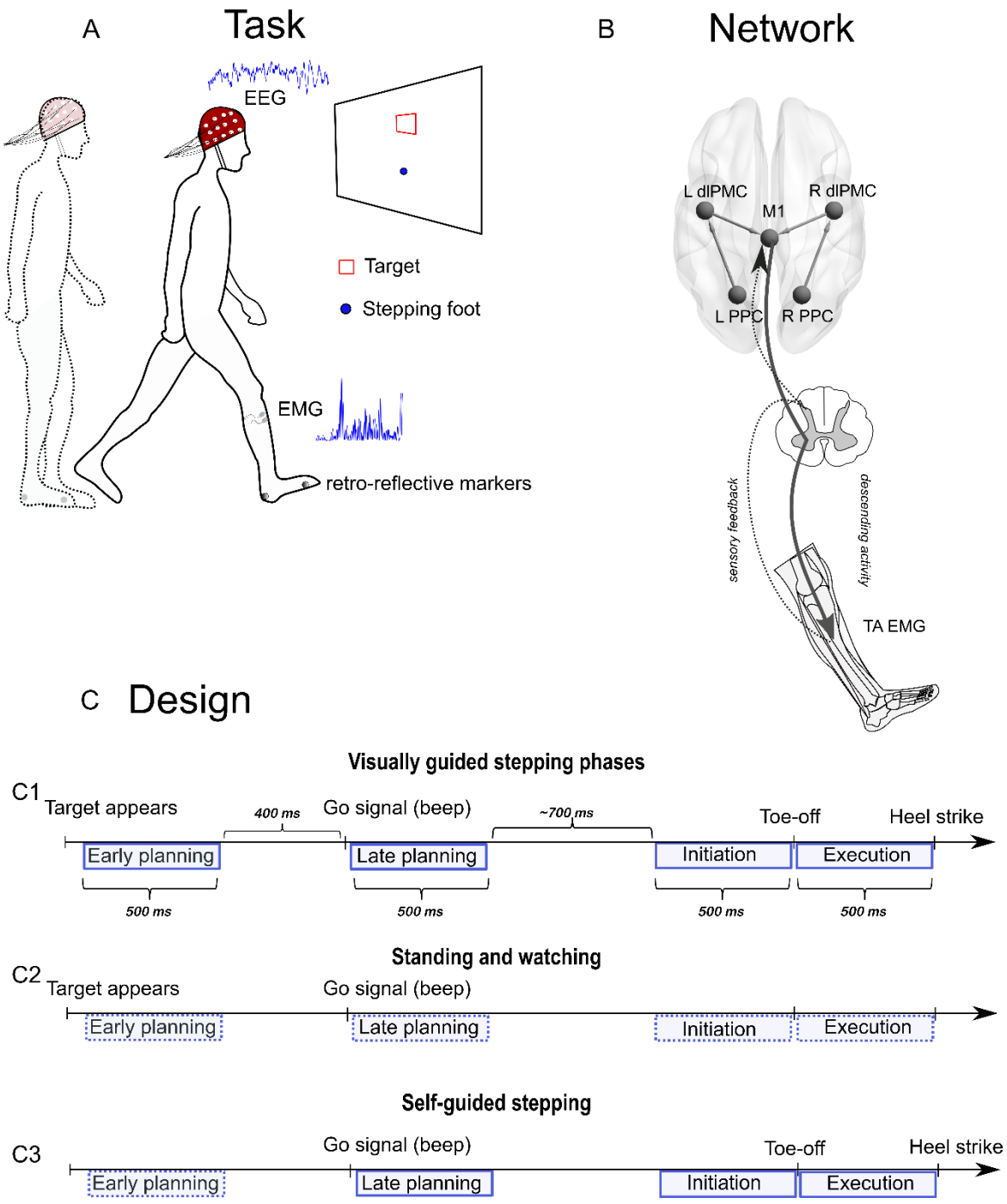

Figure 1. Experimental design. Participants performed a visually guided stepping task aiming to hit virtual visual targets (A) while EEG, EMG from the anterior tibial muscle (TA) of the stepping leg, and kinematics were recorded. We analyzed forward-directed coherence in a parieto-frontal and corticomuscular network of interest during the task (B). Coherence was quantified during four phases of the step, each with 500 ms duration (C1): early planning was the period following target presentation; late planning was the period following the go cue; initiation was period prior to toe-off, and execution was the period prior to heel-

strike (swing phase). Coherence during the visually guided stepping task was compared to two control tasks: standing and watching (C2), designed to isolate step-related connectivity, and self-guided stepping (C3), designed to isolate connectivity related to visual guidance of the step. The period between the end of late planning and beginning of the initiation phase was ~700 ms across the two stepping conditions (C1). Dotted lines in C2 and C3 show that the phases in the control tasks were chosen to temporally correspond to the phases of interest in visually guided stepping, e.g., there is no actual step initiation in the standing and watching condition. Note that sensory feedback in B is shown for physiological cohesion but was not directly investigated in this study. L; left, R; right, PPC; posterior parietal cortex, dlPMC; dorsolateral premotor cortex, M1; primary motor cortex (leg area), TA EMG; EMG from right anterior tibial muscle.

2.5.4 Source reconstruction

We performed our connectivity analysis in source space, as opposed to electrode space, because this mitigates the effect of spatial spreading of electric fields on connectivity estimates (Schoffelen and Gross 2009; Bastos and Schoffelen 2016).

We adopted a regions of interest approach to evaluate oscillatory connectivity in a sensorimotor network involved in visually guided movements. We used MNI coordinates from previous fMRI studies investigating visually guided foot movements as the centroids for our regions of interest (Christensen et al. 2007; Francis et al. 2009). Our network comprised the primary motor cortex (M1; Brodmann area 4) (represented by one source due to the medial location of the leg area), the right and left dorsolateral premotor cortex (dlPMC; Brodmann area 6), the right and left superior parietal gyrus of the posterior parietal cortex (PPC; Brodmann area 7), and the right TA (Figure 1B) (MNI to Brodmann conversion: Lacadie et al. 2008). We chose to exclude the supplementary motor area (SMA) from our network due to its close spatial proximity to the lower limb area of M1.

Table 1. MNI coordinates for centroids of cortical regions of interest. Coordinates were reversed for opposite hemisphere. M1; primary motor cortex (leg area), dlPMC; dorsolateral premotor cortex, PPC; posterior parietal cortex (superior parietal gyrus). Coordinates are from Christensen et al., 2007 and Francis et al., 2009.

Region	x (mm)	y (mm)	z (mm)
M1	-4	-26	72
R/L dlPMC	+/-42	-8	54
R/L PPC	+/-21	-63	63

Source time series were reconstructed using a 'virtual electrode' implemented in the DAiSS toolbox of SPM software (SPM12). For each time period of interest (early and late planning, initiation, and execution), time series for the five cortical sources were constructed using a linearly constrained minimum variance beamformer (LCMV).

The beamforming approach independently scans each source location of interest and computes a spatial filter (a set of weights) that quantifies each electrode's contribution to activity in the source point of interest while suppressing contributions from other sources and noise. The filter is applied to electrode data to obtain source reconstructed time series (Van Veen et al. 1997). Spatial filters were computed using the two conditions of interest together (i.e. a *common filter*), for each time period.

The filters were computed from data covariance and lead field matrices. Lead fields were constructed from a source space comprised of a grid of points centered around the MNI coordinates for each region (radius 1.5 cm, resolution 5 mm), SPM's template MRI and the Boundary Element Model as the volume conductor. A covariance matrix regularization of 5% was used. The sources were projected to their strongest orientations.

2.5.5 Coherence analysis

For our time periods, conditions, and connection pairs of interest, we computed the magnitude squared coherence as a measure of oscillatory functional connectivity. Coherence quantifies the synchronization between two signals as a function of frequency, and estimates reflect the linear phase and amplitude

relationships between signals across trials. Oscillatory synchronization between cortical regions is taken to suggest the presence of functional relationships, i.e. communication, between them (Fries 2005).

For early and late planning, initiation, and execution phases, we estimated coherence for the following signal pairs: L PPC and L dlPMC; R PPC and R dlPMC; L dlPMC and M1; R dlPMC and M1. For initiation and execution phase, we additionally estimated coherence between M1 and TA EMG. We included this analysis only for the two phases closest to the actual movement to limit the analysis to the periods of the step where TA is expected to be most active.

Coherence analysis was implemented in NeuroSpec 2.11 (www.neurospec.org) using periodogram estimates and the multi-taper method (time-halfbandwidth product=2.5, df=1 Hz).

We focused our analyses on directed connectivity estimates reflecting the forward-directed flow through the network (Kaas and Stepniewska 2016), i.e., PPC to dlPMC, dlPMC to M1, and M1 to EMG. The choice to focus the analysis on forward-directed coherence is not intended to discount the presence and importance of backward-directed communication, but to focus the analysis on the flow of information in the hierarchical structure from sensory to motor regions and motor output.

To obtain forward directed connectivity estimates, total coherence estimates were decomposed to directional components using non-parametric directionality (NPD) analysis (Halliday et al. 2016; West et al. 2020). This method determines directionality based on temporal precedence. At each frequency, the forward lagging component of coherence was extracted. This was done by applying a pre-whitening filter to the cross-spectrum, which effectively eliminates a signal's autocorrelation whilst preserving bivariate correlations. An inverse Fourier transform is then used to convert the estimate to the time domain, where it is decomposed according to lag, allowing us to separate the coherence into forward, zero lag, and backward components. The forward lagging component was then transformed back to the frequency domain, providing a forward-directed coherence estimate. Note that the instantaneous (zero-lag) coherence is ignored, which mitigates the effects of volume conduction.

NPD has been demonstrated to perform well in the face of signal-to-noise asymmetries, and in the presence of noise and instantaneous signal mixing (West et al. 2020) and has been used previously to evaluate directed coherence using EEG, EMG and LFP recordings (Jensen et al. 2019; Spedden, Jensen, et al. 2019; West et al. 2020). It has been highlighted that there can be a lack of redundancy between results from different measures of connectivity (Strahnen et al. 2021), so to address this possibility, we also provide grand average coherence spectra based on a second connectivity method for qualitative comparison (non-parametric Granger Causality; Supplementary Figure 2).

2.5.6 Surrogate analysis

Differences in factors other than phase synchronization, e.g. signal-to-noise asymmetry or source power, can lead to spurious differences in coherence (Bastos and Schoffelen 2016), which can confound comparisons between experimental conditions. One way to address this is to use nonlinear surrogate data in which the property of interest (here, phase synchronization) is disrupted or removed (Lancaster et al. 2018). We constructed surrogate data sets in which phases were randomized to disrupt any true phase synchronization by converting real data to the frequency domain; generating random phases and multiplying them with Fourier coefficients; then converting data back to the time domain (Gias 2021). This process conserves spectral power features whilst disrupting phase synchronization (Figure 2). Accordingly, the presence of a task effect both in real and surrogate data would suggest that the effect does not result from changes in phase synchrony and can be attributed to other signal characteristics such as changes in SNR. We used surrogate data sets to compare coherence estimates between tasks on the group level by constructing one surrogate data set for each participant for each condition (see below for statistics).

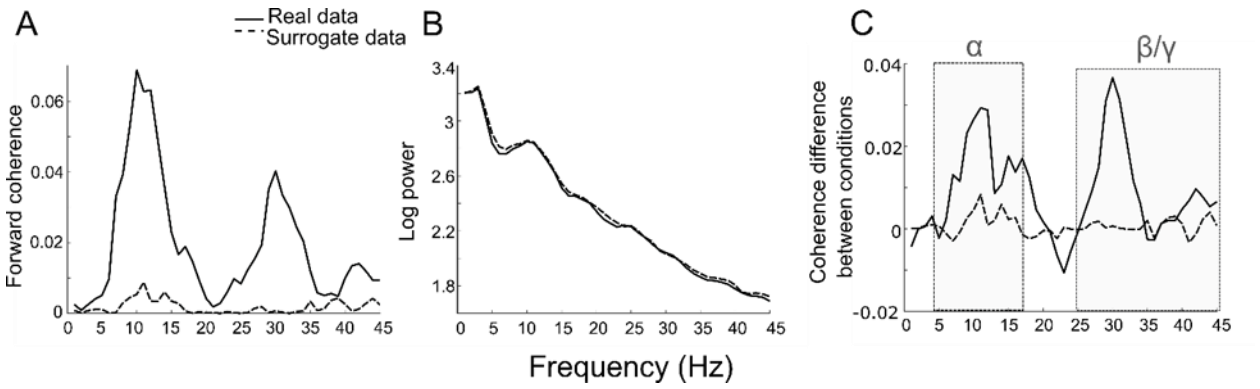

Figure 2. Surrogate data analysis. Phase-randomized surrogate data sets were constructed for each participant and each condition. Forward-directed coherence was calculated for the real data and for the phase-randomized surrogate data (A), destroying the coherence due to phase synchronization while preserving power (B). The difference in coherence between visually guided steps and the control tasks was assessed using cluster permutation, testing whether the difference between real data conditions deviated significantly from the difference between surrogate data sets for the two conditions (C). The permutation tests were performed in two a-priori defined frequency bands: alpha (5-15 Hz) and high beta/low gamma (25-45 Hz) (grey rectangles in C). Data are from a single participant.

2.5.7 Statistics

We used a non-parametric cluster permutation test (Maris et al. 2007; Gerber 2021) to evaluate whether coherence differences between conditions diverged from differences estimated from surrogate data. This corresponds to testing for an interaction effect between experimental condition and data type (real vs. surrogate). We tested two frequency bands: alpha (5-15 Hz) and high beta/low gamma (25-45 Hz). These bands were selected based on previous work studying coherence during walking (Petersen et al. 2012). Note that this is a hypothesis- (as opposed to data-) driven approach to define frequency bands, which has the advantage of being interpretable in terms of previous work and canonical frequency ranges, but also has the disadvantage of not necessarily capturing all data features.

The cluster permutation test (Maris et al. 2007) tests the null hypothesis that data from the two conditions come from the same probability distribution and is implemented as follows: For each frequency, condition differences between real and surrogate data were compared and a t-statistic was computed. Frequencies whose t-value exceeded a threshold (corresponding to 2.5 and 97.5 quantiles, two-sided paired t-test) were selected and clustered based on spectral adjacency. Cluster level statistics were computed by summing t-values in each cluster and the largest value for the cluster level statistics was taken. The significance probability for this statistic was calculated using a Monte Carlo p-value: data from both conditions were collected into one set and randomly partitioned into two sub-sets; the test statistic was calculated from the randomly partitioned data; this process was repeated 1000 times to construct a distribution; the proportion of randomly partitioned data that produced a test statistic greater than the one observed was calculated (the p-value).

We used the Benjamini-Hochberg (BH) adjustment (Benjamini and Hochberg 1995) applied to each step phase and frequency band (i.e. we corrected for 4-5 tests) and report critical p-values for each group of comparisons. For each significant cluster detected, we additionally report the mean difference in coherence between conditions across the cluster as well as Cohen's d, i.e., the mean difference divided by standard deviation of the difference across the cluster (Cohen 1988). The sign of the effect sizes indicates polarity;

positive values indicate greater coherence for visually guided stepping relative to the control task, whereas negative values indicate lower coherence for visually guided stepping relative to the control task.

We illustrated effect sizes (quantified as the mean coherence difference) in our figures by scaling the arrows indicating connections between brain regions. Arrows were only scaled for connections that exhibited statistically significant effects. For each of the two main analyses (i.e. visually guided stepping vs. standing and visually guided stepping vs. self-guided stepping) we scaled the values for all frequency bands and step phases together, so that arrow sizes can be compared across these dimensions. Brain plots were constructed using BrainNetViewer (Xia et al. 2013).

In sum, we compared estimates of lagged coherence in our parieto-frontal and corticomuscular network between experimental conditions (visually guided steps vs. standing and watching; visually guided steps vs. self-guided steps) at the four time periods (early planning; late planning; initiation; execution).

3. Results

3.1 Visually guided stepping performance

In the visually guided stepping task, participants took a single, goal-directed step aiming to place their foot precisely and hit a virtual visual target. Across participants, the median distance between foot endpoint and target in the anterior posterior direction (error) was 3.8 cm (IQR 2 cm). An overview of task performance per participant is provided in Supplementary Figure 3. Of note, one participant's performance appeared to be an extreme observation with a mean error of ~12 cm, but this data was retained after verifying that the participant had understood the task. When comparing peak acceleration during step execution (swing) between visually- and self-guided steps, we found that it did not differ significantly (paired t-test; t_{23}= -1.96, p=0.063), supporting that movements in the two conditions were executed with similar levels of vigor.

We also tested whether error was affected by leg dominancy because all participants took steps leading with the right leg. Our data demonstrated that error did not differ between participants that were right- and left leg dominant (unpaired t-test; t_{22}=0.96, p=0.346).

3.2 Taking a step: functional connectivity differs between standing and stepping

We first aimed to characterize cortico-cortical and corticomuscular connectivity patterns related to the act of taking a step. To do this, we reconstructed cortical source time series and tested whether oscillatory synchronization differed between visually guided stepping and standing and watching the same visual stimuli, in two EEG frequency bands: alpha and high beta/low gamma. The comparison was made across four phases of the step: early and late planning, initiation, and execution.

Grand average coherence spectra for the connections of interest across the four step phases are shown in Figure 3 (planning phases) and Figure 4 (movement phases). The cortico-cortical coherence spectra generally exhibited peaks at alpha, low beta, and high beta/gamma frequencies (Fig. 3A-H, Fig. 4A-J). Here, we focus our analysis on differences in alpha and high beta/gamma bands. Corticomuscular (M1 to EMG) coherence was generally low without substantial peaks, suggesting the absence of meaningful

synchronization on average (Fig.4E,J). Note that we only analyzed corticomuscular coherence for the two phases closest to the actual movement (initiation and execution) to limit the analysis to the periods of the step where TA is expected to be most active. The high coherence at low frequencies in the stepping condition (below 5 Hz) likely reflects the periodic modulation of the EMG envelope (Halliday et al. 2003).

Turning now to the progression of connectivity differences between tasks over the four phases, the following sections present results for each frequency band of interest: alpha (5-15 Hz) and high beta/low gamma (25-45 Hz).

3.2.1 Alpha band synchronization

The comparison of visually guided stepping and standing and watching suggested significant differences in coherence at alpha frequencies between tasks. We observed that alpha band coherence was down-regulated during stepping compared to standing within the cortico-cortical network, most prominently during the initiation and execution phases.

More specifically, for the planning phases, effects were sparse, with a significant down-regulation in early planning in left dlPMC to M1 coherence (critical $p=0.002$) and an absence of significant effects during late planning (critical $p=0.05$), although the left dlPMC to M1 still showed a trace of alpha desynchronization, in line with that of the early planning stage. (Fig. 3I,K).

The most widespread and largest modulations occurred during the movement initiation and execution. Alpha coherence was weakened in left PPC to dlPMC and left dlPMC to M1 during initiation (critical $p=0.007$), and in both right PPC to dlPMC and left dlPMC to M1 during execution (critical $p=0.001$) (Fig. 4K,M). Note that the most prominent effects are lateralized to the hemisphere contralateral to the stepping leg, and that ipsilateral effects become prominent in the execution phase, perhaps due to the push off of the standing leg.

M1 to EMG coherence did not exhibit significant task effects, neither during initiation nor execution. Effect sizes and cluster frequencies for this comparison are reported in Table 2.

3.2.2 High beta-low gamma synchronization

Interestingly, beta/gamma coherence exhibited both distinct and similar task-related modulations to alpha band coherence. Whereas differences between tasks were somewhat limited in the alpha band during planning, beta/gamma coherence exhibited a widespread up-regulation during early planning in stepping relative to standing (Fig. 3J). This included significant increases in left and right PPC to dlPMC as well as left dlPMC to M1 coherence (critical p=0.017). No effects were observed during late planning (critical p=0.05) (Fig. 3L). This may reflect that demands for integration of information post-cue are minimal.

During the movement phases, i.e., initiation and execution, beta/gamma coherence was down-regulated, similar to what was observed in the alpha band (Fig. 4L,N). This was manifest as a decrease during step initiation in right PPC to dlPMC and left dlPMC to M1 coherence (critical p=0.012) and during step execution in bilateral dlPMC to M1 connections and right PPC to dlPMC (critical p=0.016). As was the case for the alpha band, M1-EMG coherence did not differ between tasks. Effect sizes and cluster frequencies for this comparison are reported in Table 2.

Collectively, the act of taking a step compared to standing was characterized by (1) an initial and prevalent up-regulation of beta/gamma cortico-cortical connectivity during planning and (2) a down-modulation of both alpha and beta/gamma coherence during the movement phases, i.e., initiation and execution.

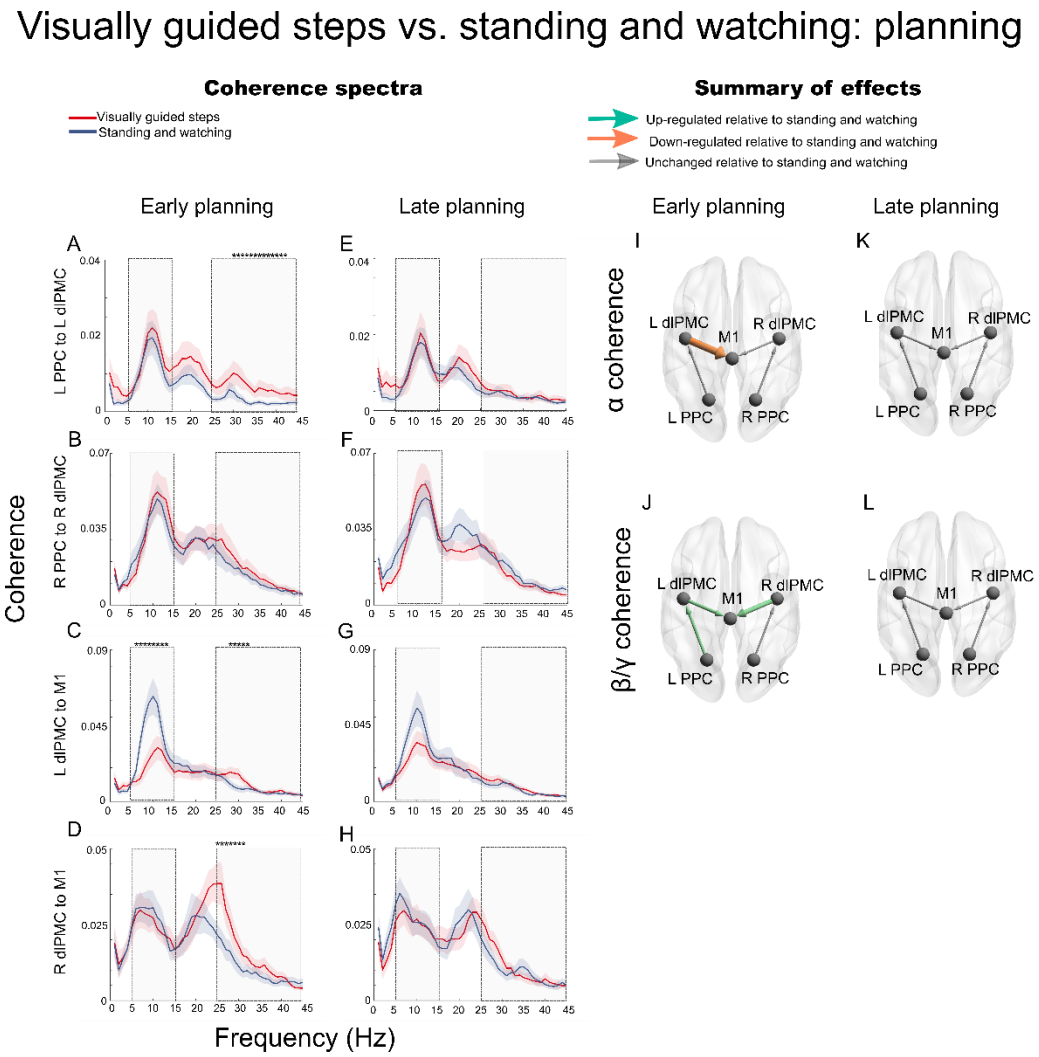

Figure 3. Visually guided stepping vs. standing and watching: planning phases. Grand mean (n = 24) coherence for visually guided steps compared to standing and watching (control) for the connections of interest during early and late planning phases (A-H). Grey rectangles indicate the frequency bands that were tested using cluster permutation for real condition difference vs. surrogate condition difference: alpha (5-15 Hz) and high beta/low gamma (25-45 Hz). * indicates statistically significant cluster (p<Benjamini Hochberg adjusted critical p-value). Means and uncertainties are bootstrapped mean and bootstrap standard error (non-normally distributed data). Statistically significant effects are summarized schematically in I-L. Arrow sizes are scaled to reflect the mean difference in coherence between conditions. L; left, R; right, PPC; posterior parietal cortex, dlPMC; dorsolateral premotor cortex, M1; primary motor cortex (leg area). Note that the coherence axes in each column of A-H are scaled differently so all data features are visible.

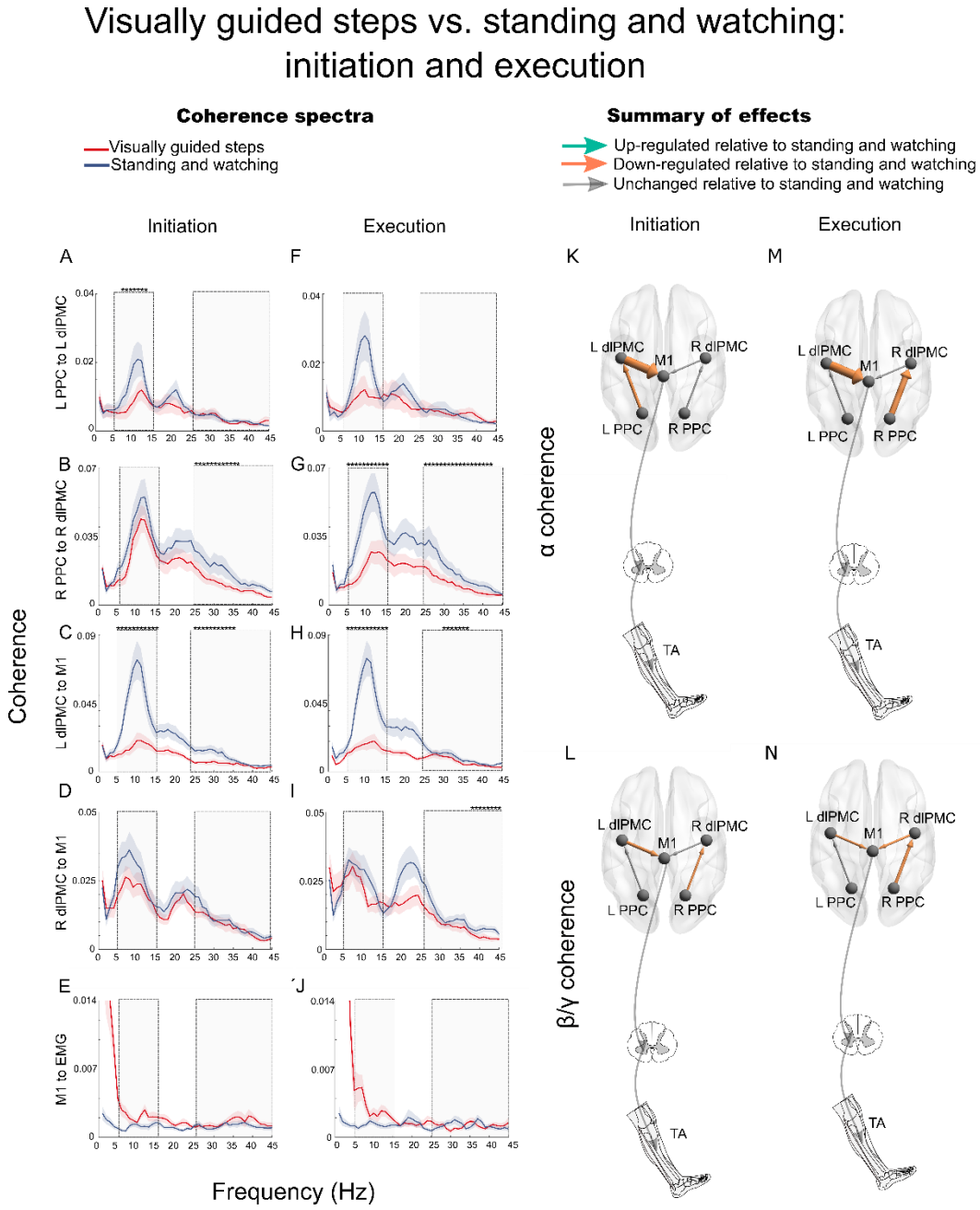

Figure 4. Visually guided stepping vs. standing and watching: movement phases. Grand mean (n = 24) coherence for visually guided steps compared to standing and watching (control) for the connections of interest during initiation and execution (swing) phases (A-J) . Grey rectangles indicate the frequency bands that were tested using cluster permutation for real condition difference vs. surrogate condition difference: alpha (5-15 Hz) and high beta/low gamma (25-45 Hz). * indicates statistically significant cluster (p<Benjamini Hochberg adjusted critical p-value). Means and uncertainties are bootstrapped mean and bootstrap standard error (non-normally distributed data). Statistically significant effects are summarized schematically in K-N.

Arrow sizes are scaled to reflect the mean difference in coherence between conditions. L; left, R; right, PPC; posterior parietal cortex, dlPMC; dorsolateral premotor cortex, M1; primary motor cortex (leg area), TA; anterior tibial muscle. Note that the coherence axes in each column of A-J are scaled differently so all data features are visible.

Step phase	Cluster frequencies and effect size		
	Alpha band		**High beta/low gamma band**
Early planning	Left PPC to dlPMC: *NS* Right PPC to dlPMC: *NS* **Left dlPMC to M1: 6-13 Hz, d=-0.91, diff.=-0.021,** Right dlPMC to M1: *NS*	Early planning	**Left PPC to dlPMC: 30-42 Hz, d=0.57, diff.=0.004** Right PPC to dlPMC: *NS* **Left dlPMC to M1: 28-32 Hz, d=0.71, diff.=0.006** **Right dlPMC to M1: 25-31 Hz, d=0.63, diff.=0.011**
Late planning	Left PPC to dlPMC: *NS* Right PPC to dlPMC: *NS* Left dlPMC to M1: *NS* Right dlPMC to M1: *NS*	Late planning	Left PPC to dlPMC: *NS* Right PPC to dlPMC: *NS* Left dlPMC to M1: *NS* Right dlPMC to M1: *NS*
Initiation	**Left PPC to dlPMC: 7-13 Hz, d=-0.58, diff.=-0.007** Right PPC to dlPMC: *NS* **Left dlPMC to M1: 5-15 Hz, d=-1.2, diff.=-0.030** Right dlPMC to M1: *NS* M1 to EMG: *NS*	Initiation	Left PPC to dlPMC: *NS* **Right PPC to dlPMC: 25-36 Hz, d=-0.60, diff.=-0.003** **Left dlPMC to M1: 25-35 Hz, d=-0.77, diff.=-0.007** Right dlPMC to M1: *NS* M1 to EMG: *NS*
Execution	Left PPC to dlPMC: *NS* **Right PPC to dlPMC: 5-15 Hz, d =-0.77, diff.=-0.020** **Left dlPMC to M1: 5-15 Hz, d=-1.25, diff.=-0.031** Right dlPMC to M1: *NS* M1 to EMG: *NS*	Execution	Left PPC to dlPMC: *NS* **Right PPC to dlPMC: 25-42 Hz, d=-0.96, diff.=-0.007** **Left dlPMC to M1: 30-36 Hz, d=-0.62, diff.=-0.003** **Right dlPMC to M1: 38-45 Hz, d=-0.73, diff.=-0.003** M1 to EMG: *NS*

Table 2. Effect sizes and cluster frequencies for the comparison of visually guided stepping to standing and watching. *NS*; non-significant, L; left, R; right, PPC; posterior parietal cortex, dlPMC; dorsolateral premotor cortex, M1; primary motor cortex (leg area). Bold indicates statistically significant results exceeding the Benjamini-Hoch corrected p-value. Effect size is reported as the mean difference in coherence between conditions in the significant cluster (diff.) and as Cohen's d.

3.3 Modifying a step: functional connectivity differs between visually- and self-guided steps

After establishing the pattern of connectivity differences related to the act of taking a step, we proceeded to address mechanisms related to how we modify a step when precise foot placement based on visual information is required. To highlight this aspect of the task, we compared visually guided stepping with self-guided stepping.

Grand average spectra for this analysis (Fig. 5 A-H, Fig. 6 A-J) were qualitatively similar to the previous comparison in terms of salient peaks in cortico-cortical connections and a lack of clear features in the corticomuscular coherence spectra. The following sections present results for each frequency band of interest: first alpha, then high beta/low gamma.

3.3.1 Alpha band synchronization

In the stages preceding the execution of the step (swing), alpha band coherence in cortico-cortical connections was down-regulated for visually guided relative to self-guided steps. This effect was present in left dlPMC to M1 for all three stages, i.e., early and late planning (Fig. 5 I,K) and initiation (Fig. 6K), and was also expressed in left PPC to dlPMC in late planning (early planning critical $p=0.001$; late planning critical $p=0.023$; initiation critical $p=0.008$). Note that these effects are lateralized to the hemisphere contralateral to the stepping leg. Subsequently, these modulations subsided; no significant task effects were present during the execution phase (critical $p=0.05$) (Fig. 6M). As was the case for the previous analysis, M1 to EMG coherence did not exhibit any task-related modulations, neither for initiation nor execution. Effect sizes and cluster frequencies for this comparison are reported in Table 3.

3.3.2 High beta-low gamma synchronization

For the beta/gamma band, task effects were limited to the planning phases (Fig. 5J,L). We observed an initial up-regulation during visually guided steps in left PPC to dlPMC coherence during early planning (critical $p=0.001$) followed by a down-regulation of right PPC to dlPMC coherence during late planning (critical $p=0.011$), while no cortico-cortical or cortico-muscular task-related modulations were expressed

in the movement phases, i.e., initiation and execution (critical p=0.05) (Fig. 6L,N). Effect sizes and cluster frequencies for this comparison are reported in Table 3.

Collectively, the requirement to adjust a step based on visual information was characterized by a cortical down-regulation of alpha coherence prior to step execution and bi-directional (both up and down) beta/gamma modulations in the planning phases. The most prominent pattern in these results is thus that task-related modulations occur in the phases preceding step execution.

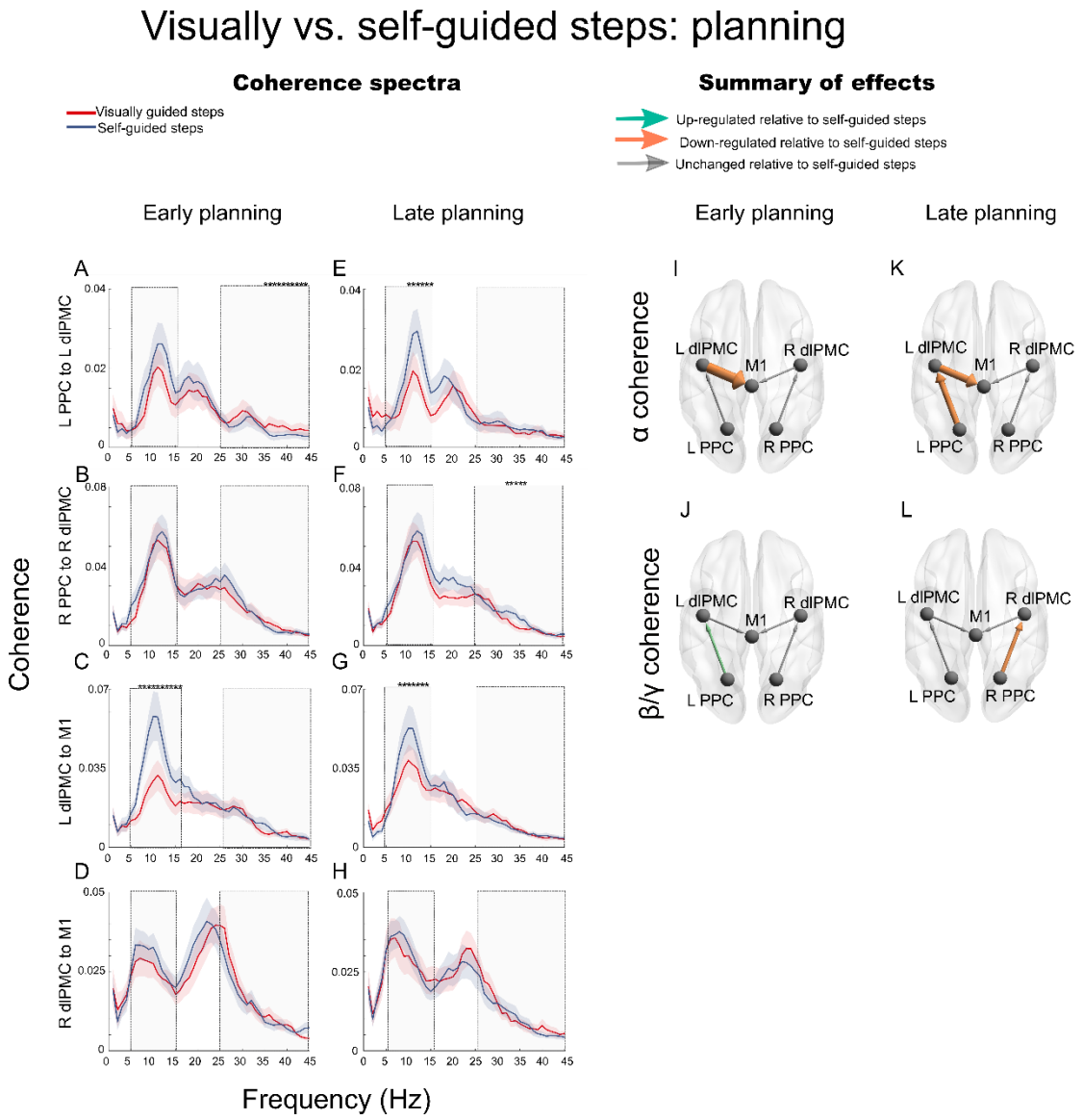

Figure 5. Visually guided stepping vs. self-guided stepping: planning phases. Grand mean (n = 24) coherence for visually guided steps compared to self-guided steps (control) for the connections of interest during early and late planning phases (A-H). Grey rectangles indicate the frequency bands that were tested using cluster permutation for real condition difference vs. surrogate condition difference: alpha (5-15 Hz) and high beta/low gamma (25-45 Hz). * indicates statistically significant cluster (p<Benjamini Hochberg adjusted critical p-value). Means and uncertainties are bootstrapped mean and bootstrap standard error (non-normally distributed data). Statistically significant effects are summarized schematically in I-L. Arrow sizes are scaled to reflect the mean difference in coherence between conditions. L; left, R; right, PPC; posterior parietal cortex, dlPMC; dorsolateral premotor cortex, M1; primary motor cortex (leg area). Note that the coherence axes in each column of A-H are scaled differently so all data features are visible.

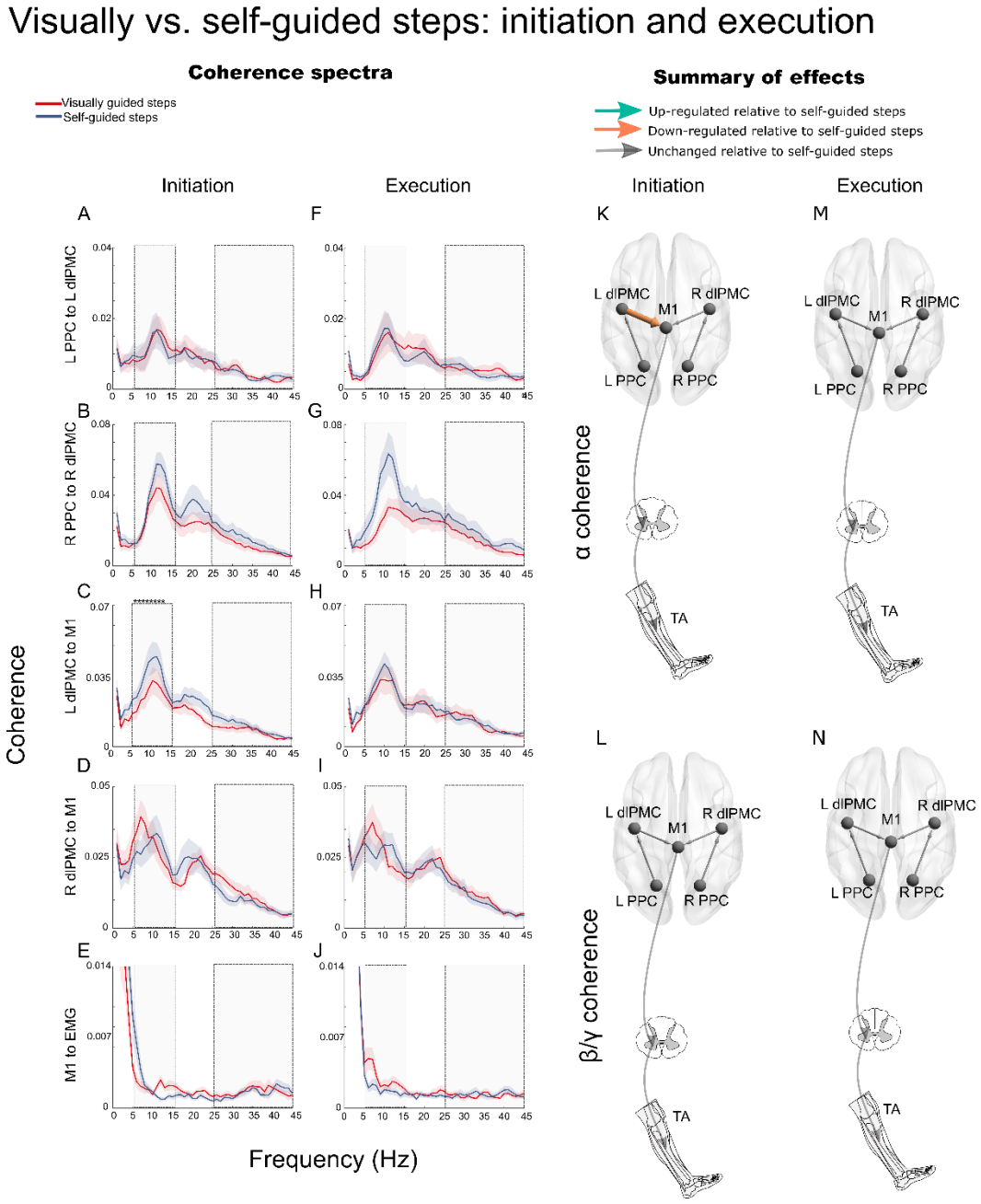

Figure 6. Visually guided stepping vs. self-guided stepping: movement phases. Grand mean (n = 24) coherence for visually guided steps compared to self-guided steps (control) for the connections of interest during initiation and execution (swing) phases (A-J). Grey rectangles indicate the frequency bands that were tested using cluster permutation for real condition difference vs. surrogate condition difference: alpha (5-15 Hz) and high beta/low gamma (25-45 Hz). * indicates statistically significant cluster (p<Benjamini Hochberg adjusted critical p-value). Means and uncertainties are bootstrapped mean and bootstrap standard error (non-normally distributed data). Statistically significant effects are summarized schematically in K-N. Arrow sizes are scaled to

reflect the mean difference in coherence between conditions.. L; left, R; right, PPC; posterior parietal cortex, dlPMC; dorsolateral premotor cortex, M1; primary motor cortex (leg area), TA; anterior tibial muscle. Note that the coherence axes in each column of A-J are scaled differently so all data features are visible.

Step phase	Cluster frequencies and effect size		
	Alpha band		**High beta/low gamma band**
Early planning	Left PPC to dlPMC: *NS* Right PPC to dlPMC: *NS* **Left dlPMC to M1: 6-15 Hz, d =-0.87, diff.= 0.018** Right dlPMC to M1: *NS*	Early planning	**Left PPC to dlPMC: 36-45 Hz, d=0.58, diff.=0.002** Right PPC to dlPMC: *NS* Left dlPMC to M1: *NS* Right dlPMC to M1: *NS*
Late planning	**Left PPC to dlPMC: 10-15 Hz, d=-0.50, diff.=-0.009** Right PPC to dlPMC: *NS* **Left dlPMC to M1: 8-14 Hz, d=-0.59, diff.= -0.012** Right dlPMC to M1: *NS*	Late planning	Left PPC to dlPMC: *NS* **Right PPC to dlPMC: 32-36 Hz, d=-0.75, diff.=-0.005** Left dlPMC to M1: *NS* Right dlPMC to M1: *NS*
Initiation	Left PPC to dlPMC: *NS* Right PPC to dlPMC: *NS* **Left dlPMC to M1: 5-12 Hz, d=-0.57, diff.=-0.010** Right dlPMC to M1: *NS* M1 to EMG: *NS*	Initiation	Left PPC to dlPMC: *NS* Right PPC to dlPMC: *NS* Left dlPMC to M1: *NS* Right dlPMC to M1: *NS* M1 to EMG: *NS*
Execution	Left PPC to dlPMC: *NS* Right PPC to dlPMC: *NS* Left dlPMC to M1: *NS* Right dlPMC to M1: *NS* M1 to EMG: *NS*	Execution	Left PPC to dlPMC: *NS* Right PPC to dlPMC: *NS* Left dlPMC to M1: *NS* Right dlPMC to M1: *NS* M1 to EMG: *NS*

Table 3. Effect sizes and cluster frequencies for the comparison of visually guided stepping to self-guided stepping**.** *NS*; non-significant, L; left, R; right, PPC; posterior parietal cortex, dlPMC; dorsolateral premotor cortex, M1; primary motor cortex (leg area). Effect size is the mean difference in coherence between conditions in the significant cluster. Effect size is reported as the mean difference in coherence between conditions in the significant cluster (diff.) and as Cohen's d.

4. Discussion

Our results demonstrated three main findings in terms of our three hypotheses: (1) The act of taking a step was characterized by an increase of cortico-cortical beta/gamma coherence during planning followed by a decrease of alpha and beta/gamma coherence during initiation and execution; (2) The adjustment of steps based on visual information was characterized by bi-directional alpha and beta/gamma modulations of cortico-cortical coherence in the phases leading up to step execution; and (3) Corticomuscular coherence did not exhibit task effects in either of the two analyses. Broadly speaking, the cortical effects differed between network couplings and according to the stage and features of the step analyzed. This context-dependent modulation of functional connectivity may reflect changing computational demands of the functional network.

The cortical network studied here has been shown to play a role in visually guided locomotion in cats and non-human primates (Drew and Marigold 2015; Marigold and Drew 2017; Takakusaki 2017; Nakajima et al. 2019). Results from a small number of fMRI studies employing imagined walking (Hamacher et al. 2015) and EEG studies employing real walking (Sipp et al. 2013; Wagner et al. 2014; Nordin et al. 2019) suggest a degree of correspondence between functional networks in humans and animals. Of interest, prior EEG work has demonstrated spectral power changes in parietal, premotor, and primary motor regions in walking tasks requiring visual guidance (Sipp et al. 2013; Wagner et al. 2014; Nordin et al. 2019), suggesting that human stepping requiring visually guided foot placement engages the regions in the network we have studied.

The present study extends this prior work mapping EEG power changes by demonstrating that functional connectivity between parietal, premotor and primary motor cortex regions is modulated in a context-dependent way: according to the stage of the stepping process, i.e., planning; initiation; execution, and according to the task feature of interest, i.e., the act of taking a step vs. modifying a step based on visual information.

4.1 Methodological considerations

A number of caveats arise when comparing cortico-cortical coherence based on EEG between experimental conditions, one of which is the problem of spurious coherence arising from differences in signal-to noise ratios and from volume conduction. We took several steps to address this issue. First, we applied beamforming as a source reconstruction technique, partly mitigating volume conduction effects (Schoffelen and Gross 2009). We also used phase-lagged coherence measures to counteract effects from signal spread, based on the fact that volume conduction effects are instantaneous and will manifest in zero-lag coherence components (Bastos and Schoffelen 2016). Finally, we used phase randomized surrogate data to confirm that condition differences were the result of differences in phase synchronization.

An important discussion in this context is the ability to disassociate differences in coherence from differences in spectral power. We aimed to account for possible effects of power differences on coherence estimates through the surrogate data analyses, focusing our results on differences in the degree of phase synchronization (Lancaster et al. 2018; see example in Figure 2). Thus, we argue that the coherence differences we observed are not caused by differences in spectral power.

In terms of possible movement artifacts affecting our data, we argue that although our tasks involved whole-body movement, the movement speeds are slow, and the trial-by-trial design allows any perturbations following the heel strike to dissipate prior to the start of the following trial. In addition, the self-guided stepping control condition involved the same degree of movement as the visually guided stepping condition, so movement-related artifacts should be fully controlled for in this comparison. Finally, we undertook a number of analytical steps when pre-processing the data to minimize the influence of these artifacts (see Methods).

It is also worth noting that we defined our frequency bands of interest based on previous work on coherence during walking (Petersen et al. 2012). This means that the frequency bands were not precisely tailored to fit our data, i.e., sometimes the frequency bands of interest did not capture the full peaks in the data.

However, we argue that based on visual inspection, the potentially overlooked differences at low beta frequencies (15-25 Hz) are in line with our existing findings and would not change our conclusions. For example, the low beta band appears to also exhibit decreases in the movement phases of stepping compared to standing (see Figure 4), which further supports our result of a broadband de-synchronization during movement.

We used a standing and watching control task aiming to isolate the act of taking a step, but we cannot exclude the possibility that participants imagined stepping towards the target during this condition. However, we did not observe robust ERD, a marker of motor imagery (Pfurtscheller 2000), during the standing task (Supplementary Figure 1), supporting that this effect did not contribute to our findings. In addition, the fact that we demonstrate differences when actual movements are performed, despite the possibility of motor imagery, argues against a large effect of participants imagining the step during standing.

Finally, it is important to point out that our work was inspired by animal studies, many of which describe single neuron firing patterns in the cortex. This approach is methodologically distinct to EEG coherence analysis, which is based on oscillations reflecting aggregate synaptic potentials in populations of many thousands of neurons. Although the precise relationship between single cell firing patterns and field potential oscillations - and its implications for coherence as a communication mechanism - is not yet well understood, existing evidence suggests that they are in any case not independent of one another (Murthy and Fetz 1996; Baker et al. 2003; Schneider et al. 2021).

4.2 Taking a step: cortico-cortical coherence differs between stepping and standing

The comparison of visually guided steps to the standing and watching condition was designed to isolate connectivity that characterizes the act of preparing and taking a step. We hypothesized that task-related modulations of connectivity in the parieto-frontal network would manifest throughout the step phases, indicating the involvement of communication within the network in both planning and execution processes.

We also expected that planning, initiation, and execution phases would exhibit distinct connectivity modulations.

Our results were in general agreement with our first hypothesis. Specifically, we found two interesting patterns of modulations with this comparison: (1) increased beta/gamma coherence during (early) planning of the visually guided step and (2) decreased alpha and beta/gamma coherence during initiation and execution.

The comparison of the two tasks during the early planning phase (just after target appearance) aimed to parse the processes related to transforming the visual information on the screen about starting foot position and target position to a motor plan in terms of body position and the required step length adjustment to hit the target. We speculate that the increase in beta/gamma coherence during early planning may reflect the integration of the sensorimotor features (Lopes da Silva 2013; Fries 2015), i.e., target placement, estimated body state, and existing motor plan, to shape the motor program for the step.

During step initiation and execution, alpha and beta/gamma coherence exhibited a widespread decrease during stepping relative to standing. The notion of movement as a broadly low synchrony state is familiar from the well-established event related desynchronization that occurs during dynamic movement (Pfurtscheller and Lopes da Silva 1999; van Wijk et al. 2012; Lopes da Silva 2013). Given that our analysis distinguishes effects due to differences in phase synchronization from effects due to possible power differences, this finding suggests that the movement phases of stepping have a broad oscillation suppressing effect that also applies to oscillatory communication.

Decreased coherence during movement is consistent with previous work on corticomuscular coherence during pinch-like tasks involving static hold phases and dynamic ramp phases. This work showed that coherence is most prominent during the steady hold phases and disappears during the dynamic ramp phases (Feige et al. 2000; Kilner et al. 2000; Baker 2007). Although this may appear at odds with findings of corticomuscular coherence during continuous treadmill walking (Petersen et al. 2012), coherence is

maximal in the mid-swing phase, where EMG activity in TA is largely tonic due to dorsiflexion in anticipation of heel strike. Corticomuscular coherence during slow walking is also generally greater than during fast walking, and coherence during static contractions is substantially larger than during walking tasks (Petersen et al. 2012). This suggests that corticomuscular coherence scales with the degree of movement dynamicity.

It is less clear how cortico-cortical functional connectivity changes during movement. In the macaque, intracranial recordings have demonstrated that local field potential synchronization between sensorimotor regions decreases during onset of dynamic wrist and finger movement (Sanes and Donoghue 1993) and arm movements towards targets (Cardoso de Oliveira et al. 2001), in general agreement with our findings. However, increased coherence during finger extensions has also been demonstrated between motor and premotor areas using ECoG in humans (Ohara et al. 2001). In addition, both increases (Toma et al. 2002) and decreases (Serrien and Brown 2002) in cortico-cortical coherence have been shown with increased speed of repetitive wrist and thumb movements using EEG.

In the context of larger scale, whole body movements in humans, a few studies have used EEG to investigate functional cortico-cortical connectivity during treadmill walking and have demonstrated a decrease in coherence/connectivity relative to standing (Wagner et al. 2013; Lau 2014; Peterson and Ferris 2019), which is in line with our findings.

Thus, while there is general agreement that spectral power and corticomuscular coherence decrease during dynamic movement, cortico-cortical coherence patterns appear to exhibit a greater task-dependency. This highlights the importance of studying whole-body tasks like stepping as distinct from traditional paradigms like reaching or finger tapping.

It is also important to highlight the absence of task-related modulations of corticomuscular coherence in our results. We expected that coherence would be greater during stepping compared to standing, indicating greater involvement of the corticospinal pathway (Petersen et al. 2012; Spedden, Choi, et al. 2019), but our

results do not support this hypothesis. There are several possible explanations for this discrepancy. The single step paradigm may have promoted more dynamic muscle contractions than during slower, steady-state treadmill walking, which would decrease the likelihood of observing corticomuscular coherence. Alternatively, the lack of effect may simply reflect a challenge in detection, seeing as coherence was generally low and without salient peaks, at least on average. In support of this, some previous work has shown that corticomuscular coherence is relatively weak and can be difficult to detect during walking (Jensen et al. 2018) without e.g. individualizing source locations or customizing frequency bands (Petersen et al. 2012). We suggest that these are the two most likely explanations, but we cannot exclude the possibility that coherence during steady-state walking may fundamentally differ from coherence as an execution signal for a single step (i.e., that reported here).

Collectively, our results suggest that the visually guided step, compared to passively standing and watching the same visual stimuli, involves an up-regulation of beta/gamma coherence during planning and an alpha and beta/gamma down-regulation during initiation and execution within the parieto-frontal network. We interpret this as indicating that communication between PPC, dlPMC and M1 is involved both in planning and movement phases of a step, and that this involvement is distinct for planning, where oscillatory communication is broadly tightened, and step execution, where oscillatory communication is relaxed.

4.3 Modifying a step: cortico-cortical coherence differs between visually and self-guided steps

The comparison between visually guided steps and self-guided steps was designed to identify connectivity related to modifying a step based on visual information. We hypothesized that step modifications based on visual information are characterized by cortical connectivity modulations in planning phases, indicating that the major involvement of this network is in the stages leading up to movement initiation. Our results broadly support this hypothesis.

We observed task effects on cortico-cortical coherence during the phases leading up to step execution, i.e., primarily in the planning phases. Effects were present in both frequency bands; alpha coherence was down-

regulated while beta/gamma connectivity was initially up- then down-regulated. However, in the initiation and execution phases, task effects in both frequency bands waned, with a complete absence of differences during execution (swing).

We interpret this as indicating that the primary cortical computational demands related to visual guidance (at least in this network) lie in the planning processes. This is broadly consistent with the ballistic model of voluntary stepping as a controlled fall in which pre-step activity sets the body's initial conditions for the step and thus controls its trajectory (Lyon and Day 2005), implying that computations during planning phases may be more critical for adjusting steps to hit a target than during step execution. This finding is also consistent with the structure of our stepping task: visual feedback of foot position was only available during planning and after heel strike, which probably discouraged online modifications of foot trajectory during swing/execution.

Like the previous analysis, we did not observe task-related modulations of corticomuscular coherence in this comparison, which was not in agreement with our hypothesis. In addition to our previous discussion points on the lack of effect on corticomuscular coherence, it is also worth noting that in some of our previous, similar studies (Jensen et al. 2018; Spedden, Choi, et al. 2019), visual feedback of foot position was available throughout the swing phase, allowing for online guidance and adjustment of trajectory. This is in contrast to the design we used in the present study, where visual feedback of foot position was not provided before heel strike. It is possible that the presence of online visual feedback contributes to the increases in coherence we observed previously (Spedden, Choi, et al. 2019).

Collectively, the results from the comparison of visually guided and self-guided stepping indicate that adjustments of step trajectory based on visual information are characterized by modulations of alpha and beta/gamma band cortico-cortical coherence in the early phases of the step, thus the major requirements for the parieto-frontal network are in the planning phase of the step.

4.4 Communication through coherence

The communication through coherence hypothesis (Fries 2005, 2015) suggests the synchronization of neural oscillations as an important mechanism for communication in distributed CNS networks. The task-related modulations we observed during visually guided steps suggest that the CNS makes use of this communication mechanism in the context of large scale, whole body movements requiring visuomotor control.

Different rhythms may play different roles in communication through coherence (Buzsaki and Draguhn 2004). We suggest that the decreases we observed in alpha band coherence might serve to increase the computational flexibility in this network. The predictable nature of oscillations as a low entropy state may limit the capacity for information processing (Baker et al. 1999; Hanslmayr et al. 2012); consequently, the decreased coherence we observed may reflect task complexity. In line with this, alpha oscillations have been suggested to contribute to tuning the excitatory/inhibitory balance (Fries 2015; Peterson and Voytek 2017). Alternatively, alpha frequencies have also been linked to attentional requirements (Palva and Palva 2007). In terms of the functional role of high beta/low gamma coherence, oscillations at these frequencies have been linked to the binding of functionally related information to form neural representations of e.g. sensory objects or motor acts (Lopes da Silva 2013). As follows, we speculate that increases in beta/gamma coherence may reflect the integration of sensorimotor task features.

Interestingly, we observed a wideband decrease in cortico-cortical coherence during movement compared to standing, suggesting that the movement itself only requires little parieto-motor synchrony. Generally, the coherence values we observed were also weak, which is in line with a large body of previous work on connectivity during large-scale, dynamic movement, in particular particular (Witham et al. 2010; Petersen et al. 2012; Lau 2014; Jensen et al. 2019). Taken together, this indicates that computations in distributed networks underlying multi-muscle, whole-body movements may not require strong oscillatory connectivity.

The task-related modulations we demonstrated suggest that communication through coherence is indeed important for these movement-related computations, but that only a small amount of functional connectivity is needed. The task effects we observed may thus reflect a subtle process of precisely tuning inter-regional communication to accomplish precision control during complex, large scale movement.

4.5 Stepping, locomotion, and reaching: similarities, differences, and implications for control mechanisms

Our paradigm is based on discrete stepping, which shares both similarities and differences with the more frequently studied steady-state walking paradigm. These distinctions have implications for the degree of overlap in neural control mechanisms and thus the generalizability of our paradigm to this behavior.

From a biomechanical perspective, both the leg movement and center of mass (COM) kinematics are comparable for the swing phase of the two behaviors (Winter 1987; Jian et al. 1993; Zhao et al. 2021). The ballistic model of stepping and walking, which informed our second hypothesis, describes the COM trajectory as a controlled fall, in which COM position and velocity are initialized prior to toe-off, then exploited to produce a specific step length and direction (Matthis et al. 2017; Day and Bancroft 2018). This suggests similar processes of step initiation and execution in the two behaviors. We speculate that the added challenge of coordinating this initialization in a dynamically instable posture during steady state walking may incur additional computational demands to spinal and subcortical circuits (Takakusaki 2017) not reflected in our network or results.

Optic flow, i.e., the apparent movement of the environment caused by relative motion between an observer and their surroundings (Rossignol 1996; Warren et al. 2001), is not well represented in our single step paradigm. It may entail greater spatial integration demands in the dorsal visual pathway during continuous walking through an environment relative to discrete stepping (Greenlee 2000). Of note, however, this limitation is also present in treadmill paradigms, which are frequently used to study walking in humans.

The rhythmicity of steady-state walking also differs from the discrete nature of goal-directed steps. It has been demonstrated that discrete movements generally require greater cortical involvement than their rhythmic counterparts (Schaal et al. 2004; Hogan and Sternad 2007; Yu et al. 2007). In the case of kinematically matched rhythmic and discrete movements, it has been shown that regions activated during the rhythmic movement were also activated during the corresponding discrete movement, but that the discrete movement was characterized by additional activation in higher cortical planning areas (Schaal et al. 2004). Consequently, we may expect the discrete stepping to engage a cortical network that overlaps with steady-state walking, and that this network is engaged to a greater degree during the discrete step.

A related and important issue is whether visually guided discrete steps are more similar to steady-state walking or visually guided reaching. The three behaviors share the similar need for precise visuomotor coordination to position the foot or hand according to objects in the environment, and work in animals has suggested similar neuronal activity underlying visually-guided gait modifications and reaching (Yakovenko and Drew 2015). However, humans walk on two legs, which incurs greater dynamic balance constraints and thus different possibilities for control strategies for locomotion and stepping compared to reaching. In reaching, the arm can move more independently of the body to reach towards the target, whereas during stepping and locomotion, a specific foot placement can be achieved by adapting the controlled fall of the COM (the 'ballistic' strategy), by modulating the push off of the opposite leg, and/or through a reaching movement with the leg (Matthis et al. 2017; Day and Bancroft 2018; Barton et al. 2019). Importantly, it has been demonstrated that humans prefer to adjust step trajectory by adapting the controlled fall of the COM, rather than performing a reaching movement with the leg, and that the former is also more effective (Barton et al. 2019). Reaching with the leg does likely represent a control strategy used under some conditions, but during natural walking, when visual information is available before step initiation, the preferred strategy appears to be tailoring the initial conditions of the movement so that the controlled fall reaches the foothold (Matthis et al. 2017; Barton et al. 2019).

Because this controlled fall appears to be a critical component of walking and stepping towards targets, but not of reaching, we suggest that our paradigm and inferences about control mechanisms are more directly transferrable to locomotion than reaching.

5. Conclusion

The results from this study demonstrate that communication between parietal, premotor, and primary motor regions is involved in planning and movement phases of a step, and that this involvement is distinct for planning, where oscillatory communication is tightened, and step execution, where oscillatory communication is relaxed. Further, when the step is modified based on visual information, our results indicate that the primary computational demands for this network are in the planning phases of the step. We interpret our results as suggesting that the brain makes use of communication through coherence in the context of large scale, dynamic whole body movements, reflecting a process of fine-tuning parieto-motor synchrony to achieve precise visuomotor control during human stepping.

6. Acknowledgments

This work was supported by the Fabrikant Vilhelm Pedersen og Hustrus mindelegat, and the Danish Ministry of Culture (FPK 2019-0044). SFF Acknowledges funding support from the NIHR supported UCLH Biomedical Research Centre. MES would like to acknowledge Louise Mejer and Mikkel Justiniano for technical assistance.

References

Andujar JÉ, Lajoie K, Drew T. 2010. A contribution of area 5 of the posterior parietal cortex to the planning of visually guided locomotion: Limb-specific and limb-independent effects. J Neurophysiol. 103:986–1006.

Baker SN. 2007. Oscillatory interactions between sensorimotor cortex and the periphery. Curr Opin Neurobiol. 17:649–655.

Baker SN, Kilner JM, Pinches EM, Lemon RN. 1999. The role of synchrony and oscillations in the motor output. Exp Brain Res. 128:109–117.

Baker SN, Pinches EM, Lemon RN. 2003. Synchronization in monkey motor cortex during a precision grip task. II. Effect of oscillatory activity on corticospinal output. J Neurophysiol. 89:1941–1953.

Barton SL, Matthis JS, Fajen BR. 2019. Control strategies for rapid, visually guided adjustments of the foot during continuous walking. Exp Brain Res. 237:1673–1690.

Bastos AM, Schoffelen JM. 2016. A tutorial review of functional connectivity analysis methods and their interpretational pitfalls. Front Syst Neurosci. 9:1–23.

Beloozerova IN, Sirota MG. 1993. The role of the motor cortex in the control of accuracy of locomotor movements in the cat. J Physiol. 461:1–25.

Benjamini Y, Hochberg Y. 1995. Controlling the False Discovery Rate : A Practical and Powerful Approach to Multiple Testing. J R Stat Soc Ser B. 57:289–300.

Buzsaki G, Draguhn A. 2004. Neuronal Oscillations in Cortical Networks. Science (80-). 304:1926–1929.

Cardoso de Oliveira S, Gribova A, Donchin O, Bergman H, Vaadia E. 2001. Neural interactions between motor cortical hemispheres during bimanual and unimanual arm movements. Eur J Neurosci. 14:1881–1896.

Chaumon M, Bishop DVM, Busch NA. 2015. A practical guide to the selection of independent components of the electroencephalogram for artifact correction. J Neurosci Methods. 250:47–63.

Christensen MS, Lundbye-Jensen J, Petersen N, Geertsen SS, Paulson OB, Nielsen JB. 2007. Watching your foot move - An fMRI study of visuomotor interactions during foot movement. Cereb Cortex. 17:1906–1917.

Cohen J. 1988. Statistical Power Analysis for the Behavioral Sciences. New York (NY): Routledge Academic.

Day BL, Bancroft MJ. 2018. Voluntary steps and gait initiation. Handb Clin Neurol. 159:107–118.

Drew T, Marigold DS. 2015. Taking the next step: Cortical contributions to the control of locomotion. Curr Opin Neurobiol. 33:25–33.

Feige B, Aertsen A, Kristeva-Feige R. 2000. Dynamic synchronization between multiple cortical motor areas and muscle activity in phasic voluntary movements. J Neurophysiol. 84:2622–2629.

Francis S, Lin X, Aboushoushah S, White TP, Phillips M, Bowtell R, Constantinescu CS. 2009. fMRI analysis of active, passive and electrically stimulated ankle dorsiflexion. Neuroimage. 44:469–479.

Fries P. 2005. A mechanism for cognitive dynamics: neuronal communication through neuronal coherence. Trends Cogn Sci. 9:474–480.

Fries P. 2015. Rhythms for Cognition: Communication through Coherence. Neuron. 88:220–235.

Friston KJ. 1994. Functional and Effective Connectivity. Hum Brain Mapp. 78:56–78.

Gerber EM. 2021. permutest [WWW Document]. URL https://www.mathworks.com/matlabcentral/fileexchange/71737-permutest

Gias C. 2021. Phase randomization [WWW Document]. URL https://www.mathworks.com/matlabcentral/fileexchange/32621-phase-randomization

Greenlee MW. 2000. Human cortical areas underlying the perception of optic flow: Brain imaging studies. Int Rev Neurobiol. 44:269–292.

Halliday DM, Conway BA, Christensen LOD, Hansen NL, Petersen NP, Nielsen JB. 2003. Functional Coupling of Motor Units is Modulated During Walking in Human Subjects. J Neurophysiol. 89:960–968.

Halliday DM, Farmer SF. 2010. On the Need for Rectification of Surface EMG. J Neurophysiol. 103:3547–3547.
Halliday DM, Senik MH, Stevenson CW, Mason R. 2016. Non-parametric directionality analysis – Extension for removal of a single common predictor and application to time series. J Neurosci Methods. 268:87–97.
Hamacher D, Herold F, Wiegel P, Hamacher D, Schega L. 2015. Brain activity during walking: A systematic review. Neurosci Biobehav Rev. 57:310–327.
Hanslmayr S, Staudigl T, Fellner MC. 2012. Oscillatory power decreases and long-term memory: The information via desynchronization hypothesis. Front Hum Neurosci. 6:1–20.
Hogan N, Sternad D. 2007. On rhythmic and discrete movements: Reflections, definitions and implications for motor control. Exp Brain Res. 181:13–30.
Hoshi E, Tanji J. 2006. Differential involvement of neurons in the dorsal and ventral premotor cortex during processing of visual signals for action planning. J Neurophysiol. 95:3596–3616.
Hoshi E, Tanji J. 2007. Distinctions between dorsal and ventral premotor areas: anatomical connectivity and functional properties. Curr Opin Neurobiol. 17:234–242.
Jensen P, Frisk R, Spedden ME, Geertsen SS, Bouyer LJ, Halliday DM, Nielsen JB. 2019. Using Corticomuscular and Intermuscular Coherence to Assess Cortical Contribution to Ankle Plantar Flexor Activity During Gait. J Mot Behav. 51:668–680.
Jensen P, Jensen NJ, Terkildsen CU, Choi JT, Nielsen JB, Geertsen SS. 2018. Increased central common drive to ankle plantar flexor and dorsiflexor muscles during visually guided gait. Physiol Rep. 6:1–11.
Jian Y, Winter DA, Ishac MG, Gilchrist L. 1993. Trajectory of the body COG and COP during initiation and termination of gait. Gait Posture. 70:2649–2652.
Kaas JH, Stepniewska I. 2016. The evolution of posterior parietal cortex and parietal-frontal networks for specific actions in primates. J Comp Neurol. 524:595–608.
Kilner JM, Baker SN, Salenius S, Hari R, Lemon RN. 2000. Human cortical muscle coherence is directly related to specific motor parameters. J Neurosci. 20:8838–8845.
Lacadie CM, Fulbright RK, Rajeevan N, Constable RT, Papademetris X. 2008. More accurate Talairach coordinates for neuroimaging using non-linear registration. Neuroimage. 42:717–725.
Lancaster G, Iatsenko D, Pidde A, Ticcinelli V, Stefanovska A. 2018. Surrogate data for hypothesis testing of physical systems. Phys Rep. 748:1–60.
Lau T. 2014. Walking reduces sensorimotor network connectivity compared to standing. J Neuroeng Rehabil. 2:189–210.
Litvak V, Eusebio A, Jha A, Oostenveld R, Barnes GR, Penny WD, Zrinzo L, Hariz MI, Limousin P, Friston KJ, Brown P. 2010. Optimized beamforming for simultaneous MEG and intracranial local field potential recordings in deep brain stimulation patients. Neuroimage. 50:1578–1588.
Lopes da Silva F. 2013. EEG and MEG: Relevance to neuroscience. Neuron. 80:1112–1128.
Lyon IN, Day BL. 2005. Predictive control of body mass trajectory in a two-step sequence. Exp Brain Res. 161:193–200.
Marigold DS, Drew T. 2017. Posterior parietal cortex estimates the relationship between object and body location during locomotion. Elife. 6:1–24.
Maris E, Schoffelen JM, Fries P. 2007. Nonparametric statistical testing of coherence differences. J Neurosci Methods. 163:161–175.
Matthis JS, Barton SL, Fajen BR. 2017. The critical phase for visual control of human walking over complex terrain. Proc Natl Acad Sci. 114:E6720–E6729.
Mullen T. 2012. NITRC: Cleanline: Tool/Resource Info [WWW Document]. URL http://www.nitrc.org/projects/cleanline
Murthy VN, Fetz EE. 1996. Synchronization of neurons during local field potential oscillations in sensorimotor cortex of awake monkeys. J Neurophysiol. 76:3968–3982.
Nakajima T, Fortier-Lebel N, Drew T. 2019. Premotor Cortex Provides a Substrate for the Temporal Transformation of Information during the Planning of Gait Modifications. Cereb Cortex. 29:4982–

5008.
Nordin AD, Hairston WD, Ferris DP. 2019. Human electrocortical dynamics while stepping over obstacles. Sci Rep. 9:1–12.
Ohara S, Mima T, Baba K, Ikeda A, Kunieda T, Matsumoto R, Yamamoto J, Matsuhashi M, Nagamine T, Hirasawa K, Hori T, Mihara T, Hashimoto N, Salenius S, Shibasaki H. 2001. Increased synchronization of cortical oscillatory activities between human supplementary motor and primary sensorimotor areas during voluntary movements. J Neurosci. 21:9377–9386.
Palva S, Palva JM. 2007. New vistas for α-frequency band oscillations. Trends Neurosci. 30:150–158.
Patla AE. 1997. Understanding the roles of vision in the control of human locomotion. Gait Posture. 5:54–69.
Petersen TH, Willerslev-Olsen M, Conway BA, Nielsen JB. 2012. The motor cortex drives the muscles during walking in human subjects. J Physiol. 590:2443–2452.
Peterson EJ, Voytek B. 2017. Alpha oscillations control cortical gain by modulating excitatory-inhibitory background activity. bioRxiv. 1–31.
Peterson SM, Ferris DP. 2019. Group-level cortical and muscular connectivity during perturbations to walking and standing balance. Neuroimage. 198:93–103.
Pfurtscheller G. 2000. Spatiotemporal ERD/ERS patterns during voluntary movement and motor imagery. Suppl Clin Neurophysiol. 53:196–198.
Pfurtscheller G, Lopes da Silva FH. 1999. Event-related EEG/MEG synchronization and desynchronization: basic principles. Clin Neurophysiol. 110:1842–1857.
Rossignol S. 1996. Visuomotor regulation of locomotion. Can J Physiol Pharmacol. 74:418–425.
Sanes JN, Donoghue JP. 1993. Oscillations in local field potentials of the primate motor cortex during voluntary movement. Proc Natl Acad Sci U S A. 90:4470–4474.
Schaal S, Sternad D, Osu R, Kawato M. 2004. Rhythmic arm movement is not discrete. Nat Neurosci. 7:1136–1143.
Schneider M, Broggini AC, Dann B, Tzanou A, Uran C, Sheshadri S, Scherberger H, Vinck M. 2021. A mechanism for inter-areal coherence through communication based on connectivity and oscillatory power. Neuron. 109:4050–4067.
Schoffelen J-M, Gross J. 2009. Source connectivity analysis with MEG and EEG. Hum Brain Mapp. 30:1857–1865.
Schubert M, Curt A, Colombo G, Berger W, Dietz V. 1999. Voluntary control of human gait: Conditioning of magnetically evoked motor responses in a precision stepping task. Exp Brain Res. 126:583–588.
Serrien DJ, Brown P. 2002. The functional role of interhemispheric synchronization in the control of bimanual timing tasks. Exp Brain Res. 147:268–272.
Sipp AR, Gwin JT, Makeig S, Ferris DP. 2013. Loss of balance during balance beam walking elicits a multifocal theta band electrocortical response. J Neurophysiol. 110:2050–2060.
Snyder KL, Kline JE, Huang HJ, Ferris DP. 2015. Independent Component Analysis of Gait-Related Movement Artifact Recorded using EEG Electrodes during Treadmill Walking. Front Hum Neurosci. 9:1–13.
Spedden ME, Choi JT, Nielsen JB, Geertsen SS. 2019. Corticospinal control of normal and visually guided gait in healthy older and younger adults. Neurobiol Aging. 78:29–41.
Spedden ME, Jensen P, Terkildsen CU, Jensen NJ, Halliday DM, Lundbye-Jensen J, Nielsen JB, Geertsen SS. 2019. The development of functional and directed corticomuscular connectivity during tonic ankle muscle contraction across childhood and adolescence. Neuroimage. 191:350–360.
Strahnen D, Kapanaiah SKT, Bygrave AM, Kätzel D. 2021. Lack of redundancy between electrophysiological measures of long-range neuronal communication. BMC Biol. 19:1–22.
Takakusaki K. 2017. Functional Neuroanatomy for Posture and Gait Control. J Mov Disord. 10:1–17.
Toma K, Mima T, Matsuoka T, Gerloff C, Ohnishi T, Koshy B, Andres F, Hallett M. 2002. Movement rate effect on activation and functional coupling of motor cortical areas. J Neurophysiol. 88:3377–3385.

Van Veen BD, Van Drongelen W, Yuchtman M, Suzuki A. 1997. Localization of brain electrical activity via linearly constrained minimum variance spatial filtering. IEEE Trans Biomed Eng. 44:867–880.
van Wijk BCM, Beek PJ, Daffertshofer A. 2012. Neural synchrony within the motor system: what have we learned so far? Front Hum Neurosci. 6:1–15.
Varghese JP, Merino DM, Beyer KB, McIlroy WE. 2016. Cortical control of anticipatory postural adjustments prior to stepping. Neuroscience. 313:99–109.
Wagner J, Solis-Escalante T, Neuper C, Scherer R, Müller-Putz G. 2013. Robot Assisted Walking Affects the Synchrony Between Premotor and Somatosensory Areas. Biomed Eng / Biomed Tech. 58:4–5.
Wagner J, Solis-Escalante T, Scherer R, Neuper C, Müller-Putz G. 2014. It's how you get there: Walking down a virtual alley activates premotor and parietal areas. Front Hum Neurosci. 8:1–11.
Warren WH, Kay BA, Zosh WD, Duchon AP, Sahuc S. 2001. Optic flow is used to control human walking. Nature. 4:213–216.
West TO, Halliday DM, Bressler SL, Farmer SF, Litvak V. 2020. Measuring directed functional connectivity using non-parametric directionality analysis: Validation and comparison with non-parametric Granger Causality. Neuroimage. 218:1–19.
Winter DA. 1987. The biomechanics and motor control of human gait. 2nd ed. Ontario (Canada): University of Waterloo Press.
Witham CL, Wang M, Baker SN. 2010. Corticomuscular coherence between motor cortex, somatosensory areas and forearm muscles in the monkey. Front Syst Neurosci. 4:1–14.
Xia M, Wang J, He Y. 2013. BrainNet Viewer: A Network Visualization Tool for Human Brain Connectomics. PLoS One. 8:1–15.
Yakovenko S, Drew T. 2015. Similar motor cortical control mechanisms for precise limb control during reaching and locomotion. J Neurosci. 35:14476–14490.
Yu H, Sternad D, Corcos DM, Vaillancourt DE. 2007. Role of hyperactive cerebellum and motor cortex in Parkinson's disease. Neuroimage. 35:222–233.
Zhao G, Grimmer M, Seyfarth A. 2021. The mechanisms and mechanical energy of human gait initiation from the lower-limb joint level perspective. Sci Rep. 11:1–12.